Author/s:
Yap, BHJ;Crawford, SA;Dagastine, RR;Scales, PJ;Martin, GJO

Title:
Nitrogen deprivation of microalgae: effect on cell size, cell wall thickness, cell strength, and resistance to mechanical disruption

Date:
2016-12-01

Citation:
Yap, B. H. J., Crawford, S. A., Dagastine, R. R., Scales, P. J. & Martin, G. J. O. (2016). Nitrogen deprivation of microalgae: effect on cell size, cell wall thickness, cell strength, and resistance to mechanical disruption. Journal of Industrial Microbiology and Biotechnology, 43 (12), pp.1671-1680. https://doi.org/10.1007/s10295-016-1848-1.

Nitrogen deprivation of microalgae: effect on cell size, cell wall thickness, cell strength, and resistance to mechanical disruption

Benjamin H. J. Yap [a], Simon A. Crawford [b], Raymond R. Dagastine [a], Peter J. Scales [a], Gregory J. O. Martin †[a]

[a] Department of Chemical and Biomolecular Engineering and [b] School of Botany, The University of Melbourne, Parkville, Victoria 3010, Australia

†Corresponding author: telephone: +61-3-8344-6613; fax: +61-3-8344-4153; e-mail: gjmartin@unimelb.edu.au

Abstract

Nitrogen deprivation (N-deprivation) is a proven strategy for triacylglyceride (TAG) accumulation in microalgae. However, its effect on the physical properties of cells and subsequently on product recovery processes is relatively unknown. In this study, the effect of N-deprivation on the cell size, cell wall thickness and mechanical strength of three microalgae was investigated. As determined by analysis of micrographs by Transmission Electron Microscopy (TEM), the average cell size and cell wall thickness for N-deprived *Nannochloropsis* sp. and *Chlorococcum* sp. were *ca.* 25% greater than the N-replete cells; and 20% and 70% greater respectively for N-deprived *Chlorella* sp. The average Young's modulus of N-deprived *Chlorococcum* sp. cells was estimated using atomic force microscopy to be 775 kPa; 30% greater than the N-replete population. Although statistically significant, these microstructural changes did not appear to affect the overall susceptibility of cells to mechanical rupture by high pressure homogenisation. This is important as it suggests that subjecting these microalgae to nitrogen starvation ~~starving these microalgae~~ to accumulate lipids does not adversely affect the recovery of intracellular lipids.

Key words

Microalgae; cell strength; nitrogen deprivation; cell rupture; atomic force microscopy

Introduction

Environmental conditions play a major role in determining the content and composition of lipids produced by microalgae [39]. Particularly important is the effect of growth conditions on the relative rates of cell division and storage lipid production [20]. Driven to adapt over a wide range of growth conditions, many species have developed the ability to efficiently modify lipid metabolism in response to various external stimuli [14,50,53]. For example, the availability of nutrients such as phosphorus [26,44,35], nitrogen [5,36,43] and silicon [38,62] have been shown to influence both lipid quantity and composition in many microalgae. Other environmental factors found to influence lipid composition include temperature [6], salinity [49,33], light intensity [12,33,56], and light cycle [8,48]. The ability to influence lipid metabolism in microalgae presents a commercial opportunity for the production of lipid-based products such as biofuel, oleochemicals and nutritive oils [58].

Triacylglyceride (TAG) oils are important lipids with application to the production of biodiesel [41] and nutraceutical oils [28]. The commercial viability of producing TAG-based products from microalgae is dependent on the productivity and cellular concentration that can be obtained. Nitrogen deprivation (N-deprivation) is a proven strategy to maximise the concentration of TAG in microalgae [50,37,20], and the ability of different algae to accumulate TAG in response to N-deprivation has been a key factor in the screening and selection of commercially suitable strains [37,21,11,5]. When microalgae are N-deprived and unable to produce new proteins for growth, biosynthetic metabolism is directed towards producing and accumulating TAG as a stored form of carbon and energy [20,50]. These TAGs are deposited as densely packed lipid bodies located within the cytoplasm of the microalgae [9].

The accumulation of TAGs during N-deprivation enables continued utilisation of light to produce new biomass from CO_2, however at a reduced overall productivity compared to growth under optimal conditions [42]. Strategies to balance this trade-off between biomass production and TAG accumulation are generally variations of a two-stage process whereby biomass concentration is increased prior to the depletion of nitrogen [37,5]. Efforts to optimise N-deprivation growth regimes

are ongoing, and have to date been primarily focussed on maximising TAG productivity. However, the effect of physical changes to the cells resulting from N-deprivation on the process efficiency of recovering of intracellular lipids from the biomass is still poorly understood.

The cell wall of microalgae and its response to changes in the growth environment is an important consideration in species selection considering it is the main barrier to the recovery of intracellular lipids [59]. The ability of microbial cells to resist mechanical rupture (e.g. by high pressure homogenisation) has been linked to the mechanical strength of the cell and the thickness of the cell wall [7,29]. An increase in cell wall thickness of up to 70% has been reported for *Chlorella emersonii* when grown in a hypersaline culture, suggesting that cell wall thickness will vary with changes in growth conditions [30]. In another detailed study, N-deprivation was shown to have large effect on the internal cell structure of *Nannochloropsis gaditana*, however changes to the cell wall or the mechanical strength of the cells were not investigated [43]. Similarly, the thickening of cell walls in *Symbiodinium* spp. from N-deprivation has been previously reported without further investigating its mechanical resistance towards disruption [23,57]. While the effects of N-depletion on cell wall thickness have not been investigated in relation to cell disruption, a previous study by Van Donk *et al*. attributed the reduced digestibility of N-deprived phytoplankton by grazers to morphological changes in the cell wall [52], suggesting an increase in the robustness of cell walls may occur during N-deprivation.

The aim of this study is to investigate the effect of N-deprivation on the cell size and cell wall thickness of three biotechnologically important marine microalgae, namely *Nannochloropsis* sp., *Chlorella* sp. and *Chlorococcum* sp., and to explore any correlation of these properties with the mechanical strength of the cells and their ability to resist mechanical rupture by high pressure homogenisation [46,19,16,15]. Transmission electron microscopy (TEM) was used to investigate changes in cell wall thickness resulting from N-deprivation. Atomic force microscope (AFM) was used to probe the mechanical strength of individual cells. AFM enables force measurements of cells in the native aqueous environment to better understand the physical response of a cell to external stresses

[27,4,54]. High pressure homogenisation was chosen as the method for mechanism cell disruption as it is a proven unit operation at scale and has been recently demonstrated to be energetically feasible for large-scale microalgal processing [60]. Here, we report for the first time the effect of N-depletion on the cell wall thickness and mechanical strength of microalgae in relation to their susceptibility to mechanical cell rupture.

Materials and methods

Microalgae cultures

Cultures of *Chlorella* sp., *Chlorococcum* sp. and *Nannochloropsis* sp. were maintained in flasks with a flat surface area of 25 cm^2 (Corning Incorporated, Corning, NY) at 20°C under a continuous low photon flux intensity of 6-10 $\mu mol.m^{-2}.s^{-1}$ provided by white fluorescent lights. Cells were maintained in a modified 'f-medium' with nutrients and trace elements in synthetic seawater [13], with compositions as previously described [31]. Subcultures were prepared every 3-4 weeks.

To perform controlled experiments involving N-deprivation, 1.5 L of each species was first grown under N-replete conditions in aerated 2 L Schott bottles at 20 °C in a light:dark cycle of 12:12 hours with a photon flux intensity of 60-70 $\mu mol.m^{-2}.s^{-1}$. The aeration provided both a source of carbon and agitation for the cells in culture. Cells were harvested at the stationary phase via centrifugation at 5000 g for 15 minutes at 20 °C (Beckman Coulter Avanti 30 bench-top centrifuge with a F0685 fixed angle rotor) and resuspended in 3-4 L of fresh medium without NO_3^-. The resuspended cultures were then equally split into N-replete (NR) and N-deplete (ND) aerated cultures, whereby 5 mM NO_3^- and 0.5 mM NO_3^- were added respectively. These cultures were then allowed to grow for 7-10 days before harvesting by centrifugation as above. The small amount of nitrate added to the ND media was included to reduce any possible shock effects, and was consumed by the cells within 2 days. The concentration of NO_3^- in the NR cultures was not growth limiting within the time of the experiment, as confirmed by a previous study [28].

Image analysis by transmission electron microscopy (TEM)

Cells were pelleted in 1.5 ml Eppendorf tubes and dispersed in 2.5% glutaraldehyde in PBS for 2 hours at room temperature after discarding the supernatant. The cells were then rinsed three times in fresh buffer for 10 minutes each before post-fixing in 1% osmium tetroxide in buffer for 1 hour. The cells were again rinsed three times in fresh buffer for ten minutes each, before being dehydrated in increasing concentrations of anhydrous ethanol of 10, 30, 50, 70, 90 and 100% v/v for 15 minutes each step. Following dehydration, the cells were infiltrated with increasing concentrations of LR White resin in ethanol consisting of 25, 50, 75 and 100% resin for six hours each step. After a second change of 100% resin, the cells were embedded in fresh resin in gelatine capsules and allowed to gently sink to the bottom to form a loose pellet. The gelatine capsules were capped to exclude air and the resin polymerised in an oven at 60 °C for 24 hours.

Embedded cells in blocks were sectioned with a diamond knife on a Leica Ultracut S microtome and ultra-thin sections (90 nm) were collected onto formvar-coated 100 mesh hexagonal copper grids. The sections on grids were sequentially stained with saturated uranyl acetate for 10 mins and Triple Lead Stain for 5 min [40] and viewed in an FEI Tecnai Spirit transmission electron microscope at 120 kV. Images were captured with a Gatan Eagle camera at a resolution of 2048 x 2048 pixels. To minimise bias towards the hypothesis examined in this paper (i.e. N-depletion increases cell size and cell wall thickness), samples were fixed and images were captured without the knowledge of the growth conditions of the cell samples.

Analyses of cell sizes and cell wall thickness were performed using ImageJ, a public-domain image processing and analysis software [34]. The cell wall thickness was measured in 3 separate places on a single cell and a total of 30 individual cells per species were measured. Data collected for each species were subjected to unpaired two-tailed *t*-tests for the difference in means (N-replete vs N-deplete) assuming unequal variance where a *p*-value of less than 0.05 was considered to be significant.

Cell disruption by high pressure homogenisation

147 Cell disruption experiments were performed using a GEA Panda2K NS1001L bench top high pressure
148 homogeniser (GEA Niro Soavi, Parma, Italy) with a nominal flow rate of 10 $L.h^{-1}$ and equipped with a
149 RE+ valve. Microalgal suspensions were processed in a single pass through the homogeniser at
150 pressures ranging from 30 to 150 MPa. Analyses of the recovered homogenates were performed
151 within three hours of homogenisation. All cell disruption tests were performed in biological
152 triplicates.
153
154 Cell rupture was quantified by cell counting due to its accuracy and reproducibility [46]. The number
155 of intact cells remaining after homogenisation was counted using a Neubauer improved
156 hemocytometer (Laboroptik Ltd., Lancing, United Kingdom) with a 100 μm chamber depth. Cell
157 counting was performed using an Olympus BX51 light microscope with a DP72 digital camera
158 attachment (Olympus, Mt. Waverly, Victoria, Australia). Cell counts were normalised between the
159 control sample (unhomogenised cell count) and zero.
160
161 *Force measurements by atomic force microscopy (AFM)*
162 The mechanical stiffness of individual *Chlorococcum* sp. cells was determined using a colloidal probe
163 in a series of cell indentations using a MFP-3D AFM (Asylum Research, Santa Barbara, California,
164 USA). Spherical silica beads of 50-80 μm in diameter (Thermo Fisher Scientific Inc., Waltham, USA)
165 were glued to the apex of a rectangular silicon cantilever (Tap150-G, Budget Sensors, Sofia,
166 Bulgaria). The spring constant of the cantilevers was determined to range from 10-15 N m^{-1} using the
167 thermal method [22]. All measurements were performed at room temperature in a modified 'f-
168 medium' in synthetic seawater with the presence or absence of NO_3^- depending on the native
169 environment of the measured sample [13].
170
171 The AFM fluid cell was fitted with a circular glass disk coated with a layer of 0.1% w/v poly-L-lysine
172 (MW: 700-100 kDa, Sigma Aldrich, Australia) for cell immobilisation, onto which the cells were
173 transferred to and allowed to settle in a single plane. Silica bead attachment onto the cantilever and
174 visualisation of cells were performed using an inverted light microscope (Nikon Eclipse TE2000-U)

attached to the AFM. The colloidal probe consisting of a silica bead attached to the cantilever was positioned above an immobilised cell that was considerably smaller than the diameter of the bead. A schematic of the experimental setup is shown in Fig. 1.The force applied to the cell was kept below 1 μN, which corresponded to an average indentation of less than 1 μm into the cells. This amount of indentation into the cell was less than 10% of the total height of the cells, a required condition to apply the Hertz model for data analysis.

The AFM records the cantilever detector photodiode voltage as a function of the piezo movement, Δl using a linear variable differential transformer (LVDT). The raw photodiode voltage is converted to cantilever deflection, Δd by scaling the photodiode detector sensitivity, which was determined from the slope of the force curve obtained by pressing the cantilever against the rigid substrate surface. The force, F was then calculated by multiplying the cantilever deflection with the spring constant, k (Equation 1).

$$F = k\Delta d \tag{1}$$

To obtain a force versus indentation curve, indentation (or deformation into the cell) was calculated by subtracting the cantilever deflection from the piezo distance (Equation 2). The contact distance was assumed to be the point at which the deflection rose above the baseline deflection force level for each force curve [4].

$$\Delta z = \Delta l - \Delta d \tag{2}$$

A Hertzian contact model approximation was applied to the force versus indentation curve to obtain the Young's modulus of individual cells. Cell stiffness is one of the most common parameters measured to investigate change in the mechanical properties of biological cells. AFM was used to indent *Chlorococcum* sp. cells grown in N-replete and N-deprived conditions to estimate the Young's modulus in order to quantify the difference in their stiffness. The Hertz model [18,24] describes the simple case of elastic deformation of two homogenous bodies touching under load. An inherent

assumption for applying the Hertz theory is the material being probed must be isotropic on the scale of the indentation, which is often not the case for living cells like microalgae. However, given that the objective of this work is to determine relative differences rather than absolute elasticity values, the Hertzian approximation is adequate. A sphere-sphere configuration for the indentation geometry is assumed in this analysis considering *Chlorococcum* sp. was found to have a circularity of >0.99 and the silica bead attached to the tip is spherical. The cells of *Chlorella* sp. and *Nannochloropsis* sp. are ellipsoid, meaning the sphere-sphere model could not be applied. This issue could not be resolved as the orientation of the cells' axes could not be controlled during the measurements. Thus for *Chlorococcum* sp. cells, the relationship between the applied load, contact radii and the displacement of elastic bodies is given by Equation (3):

$$F = \frac{4}{3} E^* R^{*1/2} \delta^{3/2} \quad (3)$$

where,

$$\frac{1}{E^*} = \frac{1-\nu_1^2}{E_1} + \frac{1-\nu_2^2}{E_2}, \frac{1}{R^*} = \frac{1}{R_1} + \frac{1}{R_2} \quad (4)$$

and F (N) is the force applied to the cell, E (Pa) is the Young's modulus in Pa, R (m) is the radius of the sphere, δ (m) is the indentation depth and ν is the Poisson's ratio. Subscripts 1 and 2 denote the silica bead (*i.e.* colloidal probe) and cell respectively. The Young's modulus, E_1 and Poisson's ratio, ν_1 for the silica bead were taken as 7.3×10^{10} Pa and 0.17 respectively [10]. Another limitation in using the Hertz model in measurements involving biological cells is that the Poisson's ratio is not available. In order to determine the Young's modulus for a cell, the Poisson ratio for *Chlorococcum* sp. was assumed to be 0.5 [47,55]. For the purpose of comparing relative values of elastic modulus in this study, it is sufficient to assume incompressibility (*i.e.* ν = 0.5) when fitting the model to experimental data. Data collected for both the N-replete and N-deplete samples of *Chlorococcum* sp. were subjected to unpaired two-tailed *t*-tests for the difference in means assuming unequal variance where a *p*-value of less than 0.05 was considered to be significant.

Results

To investigate the effect of N-deprivation on the cell size and cell wall thickness of the three microalgae, TEM images were taken (Fig. 2) and analysed. For all three microalgae there was a statistically significant ($p<0.0001$) increase in the mean cell size and cell wall thickness as a result of N-deprivation (Table). For *Nannochloropsis* sp. and *Chlorococcum* sp. both the cell size and cell wall thickness were approximately 25% greater in the ND cultures. Correspondingly, the ratios of cell wall thickness to cell size were also found to remain relatively constant for both NR and ND samples of *Nannochloropsis* sp. and *Chlorococcum* sp. For the ND *Chlorella* sp., the average cell wall was approximately 70% thicker and the average cell size only 20% larger. While there were highly statistically significant differences between the means of these parameters between NR and ND cultures, there was also considerable overlap between the populations (Fig. 3) which is expected given the cell-to-cell variability within a population, particularly between cells at different stages in the growth cycle.

The elastic response of a cell to an external force is an indicator of its mechanical strength. To determine if there was any correlation between the observed increase in cell wall thickness resulting during N-deprivation and the actual mechanical strength of the cells, compression tests via cell indentation were performed on individual cells of *Chlorococcum* sp. using an AFM. A representative force versus indentation curve and subsequent Hertzian approximation of the Young's modulus are shown in Figures 4. As mentioned in the method section, the point of contact is attributed to the rise in force above the baseline. In the inset plot (Fig. 4) one can see that force or load follows a linear relationship with the indentation raised the 3/2 power. This is consistent with describing these data with a Hertz model for this geometry. The retract portion of the AFM force curves sometime exhibit adhesion between the cell and the particle, thus the advancing portion of the AFM force curve was used for the Hertz analysis. The distributions of the of the Young's moduli between the ND and NR populations (Fig. 5) overlap due to the broadness of the destructions attributed to both physical and biological variation between cells. However, the moments of the distributions reflect that there are large statistically significant differences between the means of the two populations ($p = 0.0048$). The

mean Young's modulus of the ND population (n = 44) was approximately 30% greater than the NR population (n = 42) (775 kPa and 619 kPa respectively).

To test whether the observed changes in the average cell size, wall thickness, and for *Chloroccoum* sp. the cell mechanical strength had any effect on the susceptibility of the cells to mechanical rupture, populations of cells from NR and ND cultures were subjected to high pressure homogenisation at a range of pressures. Even though a statistically significant ($p<0.0001$) increase in cell wall thickness was observed across all three species, no difference in cell rupture behaviour was observable in the data obtained (Fig. 6). Data for *Chlorococcum* sp. was not shown as the cells were very weak and were completely broken by 35-40 MPa for both NR and ND samples. The results show *Nannochloropsis* sp. to be the most resistant to mechanical rupture, followed by *Chlorella* sp. and subsequently *Chlorococcum* sp., consistent with findings reported in a previous study [46].

Discussion

The cell walls of the microalgae investigated in this study are similar to that of higher plants in that they consist of continuous structures of biopolymeric microfibrils [2]. In contrast, the coverings of some other microalgae are rather different, for instance the scaly/plate-like coverings of microalgae such as *Isochrysis galbana* and *Tetraselmis suecica* and the silica cell coverings of diatoms. For microalgae with plant-like cells walls, such as the ones examined here, the cell wall can be considered to be an elastic structure that functions to maintain cell integrity through a combination of mechanical strength and flexibility. The fundamental components of the cell wall in the species of microalgae studied here include a microfibrillar network within a gel-like matrix of proteins, hemicelluloses and pectins [1]. The microfibrils consist of chains of monosaccharide residues and cellulose. Cell walls of representative species from the genus *Chlorella* typically consist of 44-77% neutral sugars, 4-24% uronic acids, 2-11% proteins and 2-5% glucosamine [3]. The chemical composition of cell wall could further inform about the efficacy of pre-treatments to weaken the cell wall prior to mechanical cell disruption [16,32,45], but is beyond the scope of this present study.

The elastic moduli of *Chlorococcum* sp. determined here is comparable to other microorganisms with similarly structured cell walls. For example, a previous study using the AFM determined cells of the green microalgae *Scenedesmus dimorphus* in an aqueous environment to have an elastic moduli of *ca*. 2 MPa [54]. Another eukaryotic microorganism, *S. cerevisiae*, also investigated using an AFM, was found to have an elastic modulus of 0.6 MPa, although some regions of the cell wall (i.e. the bud scar) had a significantly higher elastic modulus of 6 MPa [51]. In contrast, a much higher Young's modulus of up to 22.4 GPa has been reported for diatoms that possess rigid silica cell walls [17]. None of these studies investigated the relationship between the Young's modulus and cell wall thickness. The results of the current study show a positive correlation between the Young's modulus of the entire cell and the cell wall thickness of *Chlorococcum* sp. In addition to increased cell wall thickness, it is possible that changes to the internal structure of the cells [43] that are not accounted here could have contributed to the increase in Young's modulus. Regardless, for all three microalgae tested here, the increase in cell wall thickness and corresponding increase in the Young's modulus of the cells was not sufficient to result in an observable difference in their ability to resist mechanical rupture through high pressure homogenisation.

The independence of the susceptibility of cells to mechanical rupture on N-deprivation is an important finding. It suggests that lipid accumulation can be induced by N-deprivation without resulting in extra difficulties in breaking the cell wall to recover the intracellular lipids. These results also demonstrate that it can be difficult to establish direct links between microstructural changes and observable changes in bulk processing behaviour as the relationship is not straightforward. An example of these difficulties can be found in the previous work of Lee *et al*. where an extrapolation of the mechanical strength of a single cell was used to estimate the specific energy required to disrupt a kg of biomass (i.e. by multiplying an assumed number of cells per kg of biomass) [25]. The estimated values derived from the microstructural information in the Lee *et al*. study turned out to be vastly higher than what is actually required [61].

Despite being drawn from a limited set of data, it is perhaps notable that the relative resistance to rupture of the different species was in reverse order to the average size of the cells. This was despite a trend of decreasing cell wall thickness with decreasing cell size, and in fact also a decreasing ratio in cell wall thickness to cell size (Table). Although the strength and elasticity of the cell walls of different algae are not equal, it nonetheless suggests that cell size is an important factor in determining the ability of cells to resist rupture when passed through the narrow valve gap in a high pressure homogeniser. This could also be a factor in the lack of increased resistance to rupture shown by ND populations, which in addition to having thicker cell walls, were on average larger than the NR cells. The coincidental increase in cell size may have increased the susceptibility of the ND cells to rupture, counteracting the strengthening provided by the thicker cell walls. It is however important to also note that apart from cell size and cell wall thickness, other factors such as the overall composition of the cell wall may also contribute towards the susceptibility of the cell towards mechanical rupture. Combining these observations with other insights obtained from previous work could provide further insight into the dominant mechanism of cell breakage in a high pressure homogeniser. For instance, it has been observed that the percentage of cells ruptured does not change significantly as a function of passes through the homogeniser (ruling out biological variability within the population as a dominant factor) [46] and that cell rupture is independent of solids concentration [60].

Conclusion

Nitrogen deprivation was found to significantly increase the average cell size and wall thickness of *Nannochloropsis* sp., *Chlorella* sp. and *Chlorococcum* sp. The increased cell wall thickness was correlated to an increase in the mechanical strength of N-deprived *Chlorococcum* sp. However, the differences in microstructural properties between N-replete and N-deplete microalgae did not translate to a higher resistance to cell breakage when processed through high pressure homogenisation. This result is particularly important for the development of growth regimes optimised to maximise lipid productivity through nitrogen starvation, as it indicates that cell rupture is not likely to be significantly affected for these algae.

Acknowledgments

The authors gratefully acknowledge the support of the Particulate Fluids Processing Centre, a Special Research Centre of the Australian Research Council. This work was performed in part at the Melbourne Centre for Nanofabrication (MCN) in the Victorian Node of the Australian National Fabrication Facility (ANFF) and in the Materials Characterization and Fabrication Platform (MCFP) at the University of Melbourne.

References

1. Barsanti L, Gualtieri P (2006) Algae: Anatomy, Biochemistry, and Biotechnology. CRC Press, Taylor & Francis Group, Boca Raton, FL
2. Berner T (1993) Ultrastructure of microalgae. CRC Press, Inc., Boca Raton, FL
3. Blumreisinger M, Meindl D, Loos E (1983) Cell wall composition of chlorococcal algae. Phytochemistry 22:1603-1604. doi:10.1016/0031-9422(83)80096-x
4. Bowen WR, Lovitt RW, Wright CJ (2000) Application of atomic force microscopy to the study of micromechanical properties of biological materials. Biotechnology letters 22:893-903. doi:10.1023/a:1005604028444
5. Breuer G, Lamers PP, Martens DE, Draaisma RB, Wijffels RH (2012) The impact of nitrogen starvation on the dynamics of triacylglycerol accumulation in nine microalgae strains. Bioresource Technology. doi:10.1016/j.biortech.2012.08.003
6. Converti A, Casazza AA, Ortiz EY, Perego P, Del Borghi M (2009) Effect of temperature and nitrogen concentration on the growth and lipid content of Nannochloropsis oculata and Chlorella vulgaris for biodiesel production. Chemical Engineering and Processing: Process Intensification 48:1146-1151. doi:10.1016/j.cep.2009.03.006
7. Engler C (1985) Disruption of microbial cells. In: Moo-Young M (ed) Comprehensive Biotechnology. Pegamon Press, Oxford, England,

8. Fábregas J, Maseda A, Domínguez A, Ferreira M, Otero A (2002) Changes in the cell composition of the marine microalga, Nannochloropsis gaditana, during a light:dark cycle. Biotechnology letters 24:1699-1703. doi:10.1023/a:1020661719272

9. Goold H, Beisson F, Peltier G, Li-Beisson Y (2015) Microalgal lipid droplets: composition, diversity, biogenesis and functions. Plant Cell Rep 34:545-555. doi:10.1007/s00299-014-1711-7

10. Greaves GN, Greer A, Lakes R, Rouxel T (2011) Poisson's ratio and modern materials. Nature materials 10:823-837

11. Griffiths M, van Hille R, Harrison S (2011) Lipid productivity, settling potential and fatty acid profile of 11 microalgal species grown under nitrogen replete and limited conditions. Journal of Applied Phycology:1-13. doi:10.1007/s10811-011-9723-y

12. Guihéneuf F, Mimouni V, Ulmann L, Tremblin G (2009) Combined effects of irradiance level and carbon source on fatty acid and lipid class composition in the microalga Pavlova lutheri commonly used in mariculture. J Exp Mar Biol Ecol 369:136-143. doi:http://dx.doi.org/10.1016/j.jembe.2008.11.009

13. Guillard RRL, Ryther JH (1962) Studies of marine planktonic diatoms. I. Cyclotella nana Hustedt, and Detonula confervacea (cleve) Gran. Canadian journal of microbiology 8:229-239

14. Guschina IA, Harwood JL (2006) Lipids and lipid metabolism in eukaryotic algae. Progress in Lipid Research 45:160-186. doi:DOI: 10.1016/j.plipres.2006.01.001

15. Halim R, Gladman B, Danquah MK, Webley PA (2011) Oil extraction from microalgae for biodiesel production. Bioresource Technology 102:178-185. doi:http://dx.doi.org/10.1016/j.biortech.2010.06.136

16. Halim R, Webley PA, Martin GJ (2015) The CIDES process: Fractionation of concentrated microalgal paste for co-production of biofuel, nutraceuticals, and high-grade protein feed. Algal Research
17. Hamm CE, Merkel R, Springer O, Jurkojc P, Maier C, Prechtel K, Smetacek V (2003) Architecture and material properties of diatom shells provide effective mechanical protection. Nature 421:841-843
18. Hertz H (1881) On the contact of elastic solids. J reine angew Math 92:156-171
19. Hu Q, Kurano N, Kawachi M, Iwasaki I, Miyachi S (1998) Ultrahigh-cell-density culture of a marine green alga Chlorococcum littorale in a flat-plate photobioreactor. Applied microbiology and biotechnology 49:655-662
20. Hu Q, Sommerfield M, Jarvis E, Ghirardi M, Posewitz M, Seibert M, Darzins A (2008) Microalgal triacylglycerols as feedstocks for biofuel production: perspectives and advances. Plant J 54:621-639
21. Huerlimann R, de Nys R, Heimann K (2010) Growth, lipid content, productivity, and fatty acid composition of tropical microalgae for scale-up production. Biotechnology and Bioengineering 107:245-257. doi:10.1002/bit.22809
22. Hutter JL, Bechhoefer J (1993) Calibration of atomic-force microscope tips. Review of Scientific Instruments 64:1868-1873
23. Jiang PL, Pasaribu B, Chen CS (2014) Nitrogen-deprivation elevates lipid levels in Symbiodinium spp. by lipid droplet accumulation: Morphological and compositional analyses. PLoS ONE 9. doi:10.1371/journal.pone.0087416
24. Johnson K (1985) Normal contact of elastic solids: Hertz theory. Contact mechanics:84-106

415 25. Lee AK, Lewis DM, Ashman PJ (2013) Force and energy requirement for microalgal cell
416 disruption: an atomic force microscope evaluation. Bioresource Technology 128:199-
417 206
418 26. Liang K, Zhang Q, Gu M, Cong W (2013) Effect of phosphorus on lipid accumulation in
419 freshwater microalga Chlorella sp. Journal of Applied Phycology 25:311-318.
420 doi:10.1007/s10811-012-9865-6
421 27. Lulevich V, Zink T, Chen HY, Liu FT, Liu G (2006) Cell mechanics using atomic force
422 microscopy-based single-cell compression. Langmuir 22:8151-8155
423 28. Martin GJO, Hill DRA, Olmstead ILD, Bergamin A, Shears MJ, Dias DA, Kentish SE,
424 Scales PJ, Botté CY, Callahan DL (2014) Lipid Profile Remodeling in Response to
425 Nitrogen Deprivation in the Microalgae Chlorella sp. (Trebouxiophyceae) and
426 Nannochloropsis sp. (Eustigmatophyceae). PLoS ONE 9:e103389.
427 doi:10.1371/journal.pone.0103389
428 29. Middelberg APJ (1995) Process-scale disruption of microorganisms. Biotechnology
429 Advances 13:491-551
430 30. Munns R, Greenway H, Setter T, Kuo J (1983) Turgor pressure, volumetric elastic
431 modulus, osmotic volume and ultrastructure of Chlorella emersonii grown at high and
432 low external NaCl. Journal of Experimental Botany 34:144-155
433 31. Olmstead ILD, Hill DRA, Dias DA, Jayasinghe NS, Callahan DL, Kentish SE, Scales PJ,
434 Martin GJO (2013) A quantitative analysis of microalgal lipids for optimization of
435 biodiesel and omega-3 production. Biotechnology and Bioengineering.
436 doi:10.1002/bit.24844
437 32. Olmstead ILD, Kentish SE, Scales PJ, Martin GJO (2013) Low solvent, low temperature
438 method for extracting biodiesel lipids from concentrated microalgal biomass.
439 Bioresource Technology 148:615 - 619

440 33. Pal D, Khozin-Goldberg I, Cohen Z, Boussiba S (2011) The effect of light, salinity, and
441 nitrogen availability on lipid production by Nannochloropsis sp. Applied
442 microbiology and biotechnology:1-13
443 34. Rasband WS (1997) ImageJ. National Institute of Health.
444 35. Řezanka T, Lukavský J, Nedbalová L, Sigler K (2011) Effect of nitrogen and phosphorus
445 starvation on the polyunsaturated triacylglycerol composition, including positional
446 isomer distribution, in the alga Trachydiscus minutus. Phytochemistry 72:2342-2351.
447 doi:10.1016/j.phytochem.2011.08.017
448 36. Richardson B, Orcutt D, Schwertner H, Martinez CL, Wickline HE (1969) Effects of
449 nitrogen limitation on the growth and composition of unicellular algae in continuous
450 culture. Applied microbiology 18:245-250
451 37. Rodolfi L, Chini Zittelli G, Bassi N, Padovani G, Biondi N, Bonini G, Tredici MR (2008)
452 Microalgae for oil: strain selection, induction of lipid synthesis and outdoor mass
453 cultivation in a low-cost photobioreactor. Biotechnology and Bioengineering
454 102:100-112
455 38. Roessler PG (1988) Changes in the activities of various lipid and carbohydrate
456 biosynthetic enzymes in the diatom Cyclotella cryptica in response to silicon
457 deficiency. Archives of Biochemistry and Biophysics 267:521-528.
458 doi:http://dx.doi.org/10.1016/0003-9861(88)90059-8
459 39. Roessler PG (1990) Environmental control of glycerolipid metabolism in microalgae:
460 Commercial implications and future research directions. Journal of Phycology
461 26:393-399. doi:10.1111/j.0022-3646.1990.00393.x
462 40. Sato T (1968) A Modified Method for Lead Staining of Thin Sections. Journal of
463 Electron Microscopy 17:158-159

464 41. Scott SA, Davey MP, Dennis JS, Horst I, Howe CJ, Lea-Smith DJ, Smith AG (2010)
465 Biodiesel from algae: challenges and prospects. Current Opinion in Biotechnology
466 21:277-286
467 42. Sheehan J, Dunahay T, Benemann J, Roessler P (1998) A Look Back at the US
468 Department of Energy's Aquatic Species Program: Biodiesel from Algae. In, vol 328.
469 43. Simionato D, Block MA, La Rocca N, Jouhet J, Maréchal E, Finazzi G, Morosinotto T
470 (2013) The response of Nannochloropsis gaditana to nitrogen starvation includes de
471 novo biosynthesis of triacylglycerols, a decrease of chloroplast galactolipids, and
472 reorganization of the photosynthetic apparatus. Eukaryotic Cell 12:665-676
473 44. Siron R, Giusti G, Berland B (1989) Changes in the fatty acid composition of
474 Phaeodactylum tricornutum and Dunaliella tertiolecta during growth and under
475 phosphorus deficiency. Marine ecology progress series Oldendorf 55:95-100
476 45. Spiden EM, Scales PJ, Yap BH, Kentish SE, Hill DR, Martin GJ (2015) The effects of
477 acidic and thermal pretreatment on the mechanical rupture of two industrially relevant
478 microalgae: Chlorella sp. and Navicula sp. Algal Research 7:5-10
479 46. Spiden EM, Yap BH, Hill DR, Kentish SE, Scales PJ, Martin GJ (2013) Quantitative
480 evaluation of the ease of rupture of industrially promising microalgae by high
481 pressure homogenization. Bioresource Technology
482 47. Stenson JD, Thomas CR, Hartley P (2009) Modelling the mechanical properties of yeast
483 cells. Chemical engineering science 64:1892-1903. doi:10.1016/j.ces.2009.01.016
484 48. Sukenik A, Carmeli Y (1990) Lipid Synthesis and Fatty Acid Composition in
485 *Nannochloropsis* sp. (Eustigmatophyceae) Grown in a Light-Dark Cycle. J Phycol
486 26:463-469. doi:10.1111/j.0022-3646.1990.00463.x

487 49. Takagi M, Yoshida T (2006) Effect of salt concentration on intracellular accumulation of
488 lipids and triacylglyceride in marine microalgae Dunaliella cells. Journal of
489 bioscience and bioengineering 101:223-226
490 50. Thompson Jr. GA (1996) Lipids and membrane function in green algae. Biochim Biophys
491 Acta 1302:17-45
492 51. Touhami A, Nysten B, Dufrêne YF (2003) Nanoscale Mapping of the Elasticity of
493 Microbial Cells by Atomic Force Microscopy. Langmuir 19:4539-4543.
494 doi:10.1021/la034136x
495 52. Van Donk E, Lurling M, Hessen D, Lokhorst G (1997) Altered cell wall morphology in
496 nutrient-deficient phytoplankton and its impact on grazers. Limnology and
497 Oceanography:357-364
498 53. Wada H, Murata N (1998) Membrane lipids in cyanobacteria. In: Lipids in
499 photosynthesis: structure, function and genetics. Springer, pp 65-81
500 54. Warren K, Mpagazehe J, LeDuc P, Higgs III C (2014) Probing the elastic response of
501 microalga Scenedesmus dimorphus in dry and aqueous environments through atomic
502 force microscopy. Applied Physics Letters 105:163701
503 55. Wei C, Lintilhac PM (2007) Loss of stability: a new look at the physics of cell wall
504 behavior during plant cell growth. Plant Physiology 145:763-772
505 56. Weldy CS, Huesemann M (2007) Lipid production by Dunaliella salina in batch culture:
506 effects of nitrogen limitation and light intensity. US Department of Energy Journal of
507 Undergraduate Research 7:115–122
508 57. Weng LC, Pasaribu B, Lin IP, Tsai CH, Chen CS, Jiang PL (2014) Nitrogen deprivation
509 induces lipid droplet accumulation and alters fatty acid metabolism in symbiotic
510 dinoflagellates isolated from Aiptasia pulchella. Scientific Reports 4.
511 doi:10.1038/srep05777

512 58. Wijffels RH, Barbosa MJ, Eppink MH (2010) Microalgae for the production of bulk
513 chemicals and biofuels. Biofuels, Bioproducts and Biorefining 4:287-295
514 59. Yap BHJ, Crawford SA, Dumsday GJ, Scales PJ, Martin GJO (2014) A mechanistic
515 study of algal cell disruption and its effect on lipid recovery by solvent extraction.
516 Algal Res 5:112-120
517 60. Yap BHJ, Dumsday GJ, Scales PJ, Martin GJO (2015) Energy evaluation of algal cell
518 disruption by high pressure homogenisation. Bioresource Technology 184:280-285.
519 doi:http://dx.doi.org/10.1016/j.biortech.2014.11.049
520 61. Yap BHJ, Martin GJO, Scales PJ (2016) Rheological manipulation of flocculated algal
521 slurries to achieve high solids processing. Algal Res 14:1-8.
522 doi:http://dx.doi.org/10.1016/j.algal.2015.12.007
523 62. Yu E, Zendejas F, Lane P, Gaucher S, Simmons B, Lane T (2009) Triacylglycerol
524 accumulation and profiling in the model diatoms Thalassiosira pseudonana and
525 Phaeodactylum tricornutum (Baccilariophyceae) during starvation. J Appl Phycol
526 21:669-681. doi:10.1007/s10811-008-9400-y

527

528

Fig. 1 A schematic of the experimental setup for the compression of a microalgae cell using a colloidal probe in an AFM (not to scale)

Fig. 2 Representative TEM micrographs of *Nannochloropsis* sp., *Chlorella* sp. and *Chlorococcum* sp. grown in N-replete and N-deplete conditions. Scale bars for the cell wall and whole cell micrographs for *Nannochoropsis* sp and *Chlorella* sp. indicate 100 nm and 1 μm respectively. Scale bars for the cell wall and whole cell micrographs of *Chlorococcum* sp. represent 200 nm and 2 μm respectively

Fig. 3 Histograms comparing the cell wall thickness and cell size of N-replete (NR) and N-deplete (ND) cultures of *Nannochloropsis* sp. (A, B), *Chlorella* sp. (C, D) and *Chlorococcum* sp (E, F). Mean values are presented in the Table

Fig. 4 A representative force versus indentation curve for a *Chlorococcum* sp. cell and a Hertzian sphere-sphere contact model approximation applied to the data (inset plot). Young's modulus of a cell, E_2 is obtained through the slope of the curve that is represented by the term $\frac{4}{3}\boldsymbol{E}^{*}\boldsymbol{R}^{*\mathbf{1/2}}$ (see: Equation 3). An R^2 of 0.996 was obtained for the curve represented here.

Fig. 5 Histogram comparing the Young's moduli of N-replete (NR) and N-deplete (ND) *Chlorococcum* sp. cells. Mean Young's modulus for NR and ND cells are 619 ± 292 kPa and 775 ± 200 kPa respectively (difference between means *p*-value = 0.0048).

Fig. 6 Cell rupture as a function of pressure for a single homogenising pass for (A) *Chlorella* sp. and (B) *Nannochloropsis* sp. grown in N-replete (NR) and N-deplete (ND) conditions. Error bars represent the standard deviation of triplicate experiments performed on separate algal cultures.

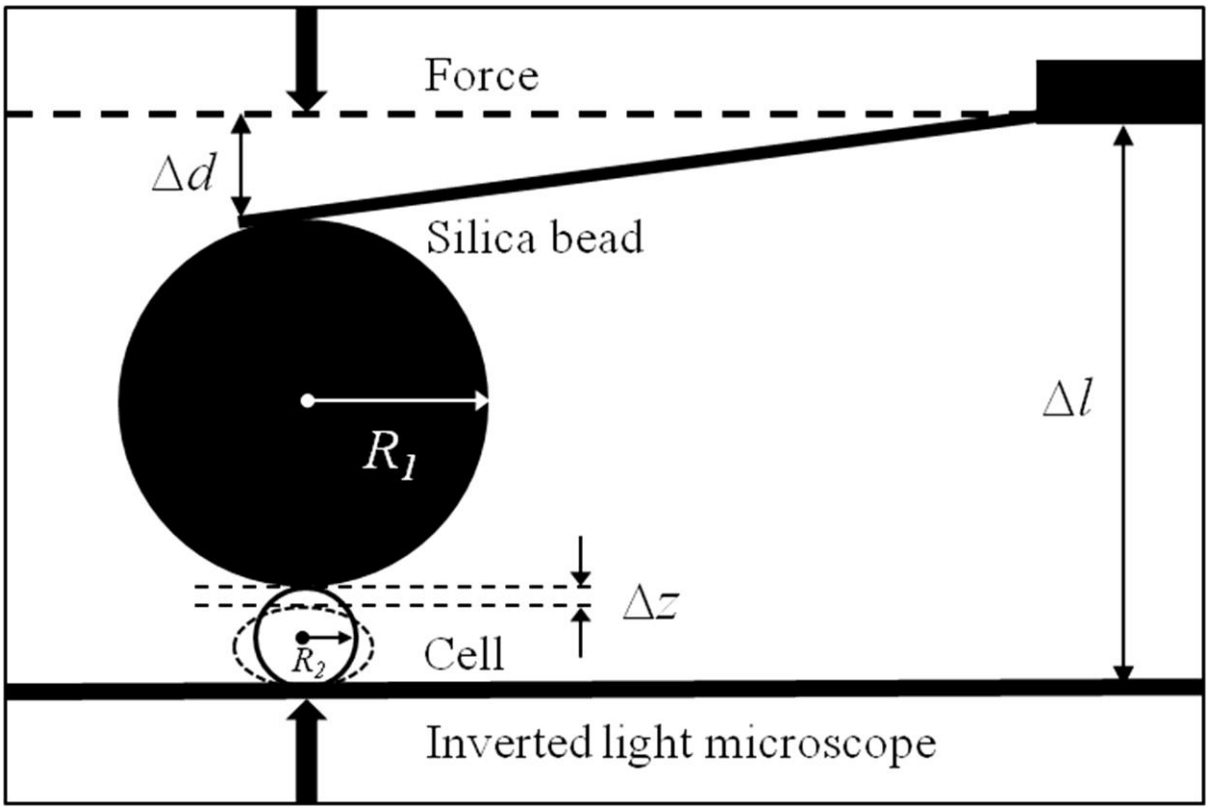
Force
Δd
Silica bead
R1
Δl
Δz
R2
Cell
Inverted light microscope

554

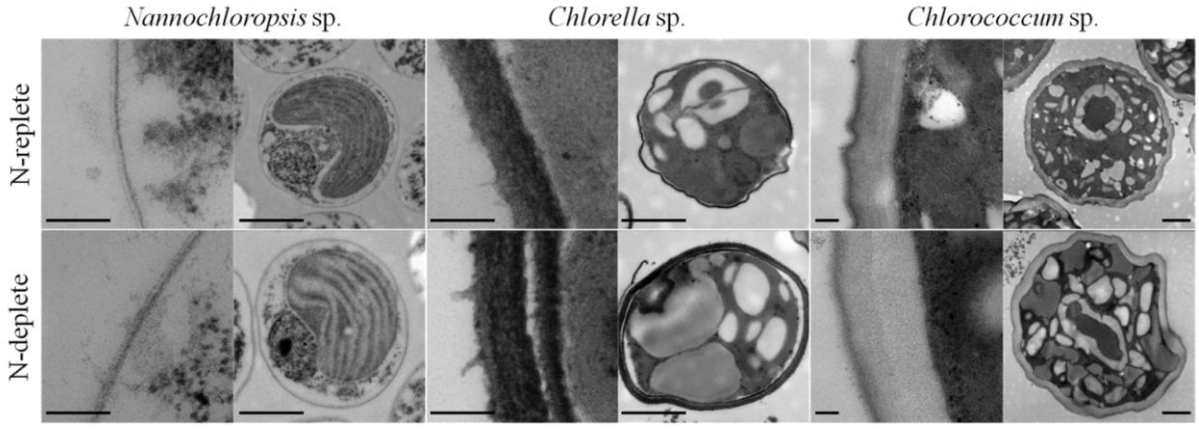
Nannochloropsis sp.
Chlorella sp.
Chlorococcum sp.
N-replete
N-deplete

555

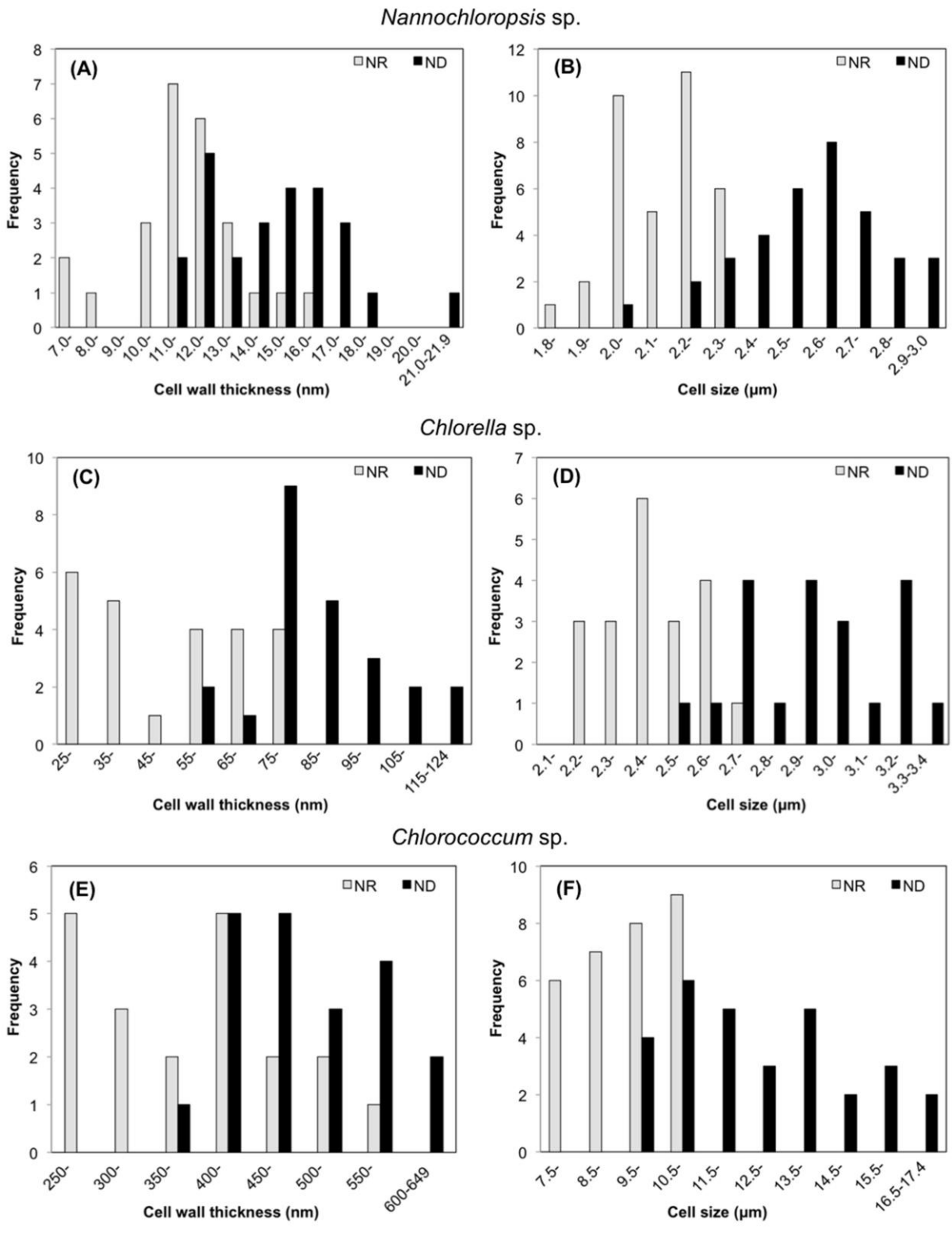
Nannochloropsis sp.
(A)
NR
ND
Frequency
Cell wall thickness (nm)
7.0-
8.0-
9.0-
10.0-
11.0-
12.0-
13.0-
14.0-
15.0-
16.0-
17.0-
18.0-
19.0-
20.0-
21.0-21.9
(B)
Cell size (µm)
1.8-
1.9-
2.0-
2.1-
2.2-
2.3-
2.4-
2.5-
2.6-
2.7-
2.8-
2.9-3.0
Chlorella sp.
(C)
25-
35-
45-
55-
65-
75-
85-
95-
105-
115-124
(D)
2.1-
2.2-
2.3-
2.4-
2.5-
2.6-
2.7-
2.8-
2.9-
3.0-
3.1-
3.2-
3.3-3.4
Chlorococcum sp.
(E)
250-
300-
350-
400-
450-
500-
550-
600-649
(F)
7.5-
8.5-
9.5-
10.5-
11.5-
12.5-
13.5-
14.5-
15.5-
16.5-17.4

556

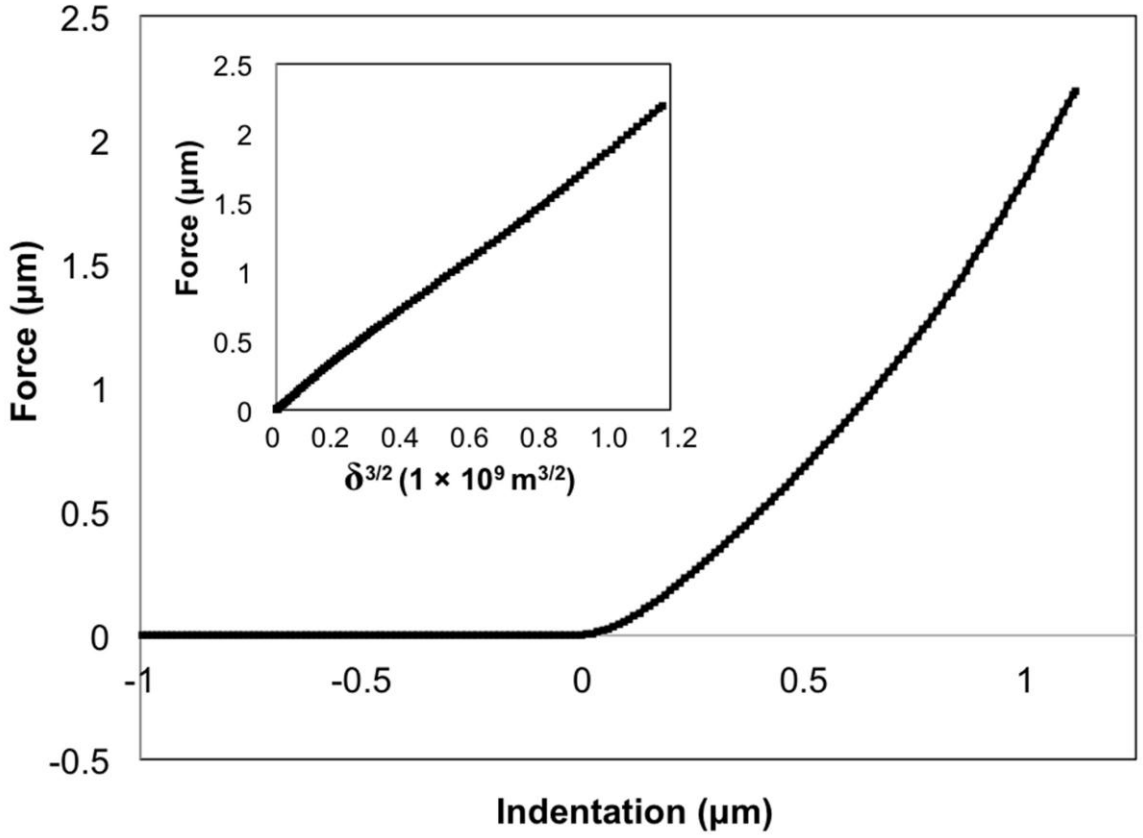
Force (μm)
Indentation (μm)
δ3/2 (1 × 10⁹ m3/2)

557

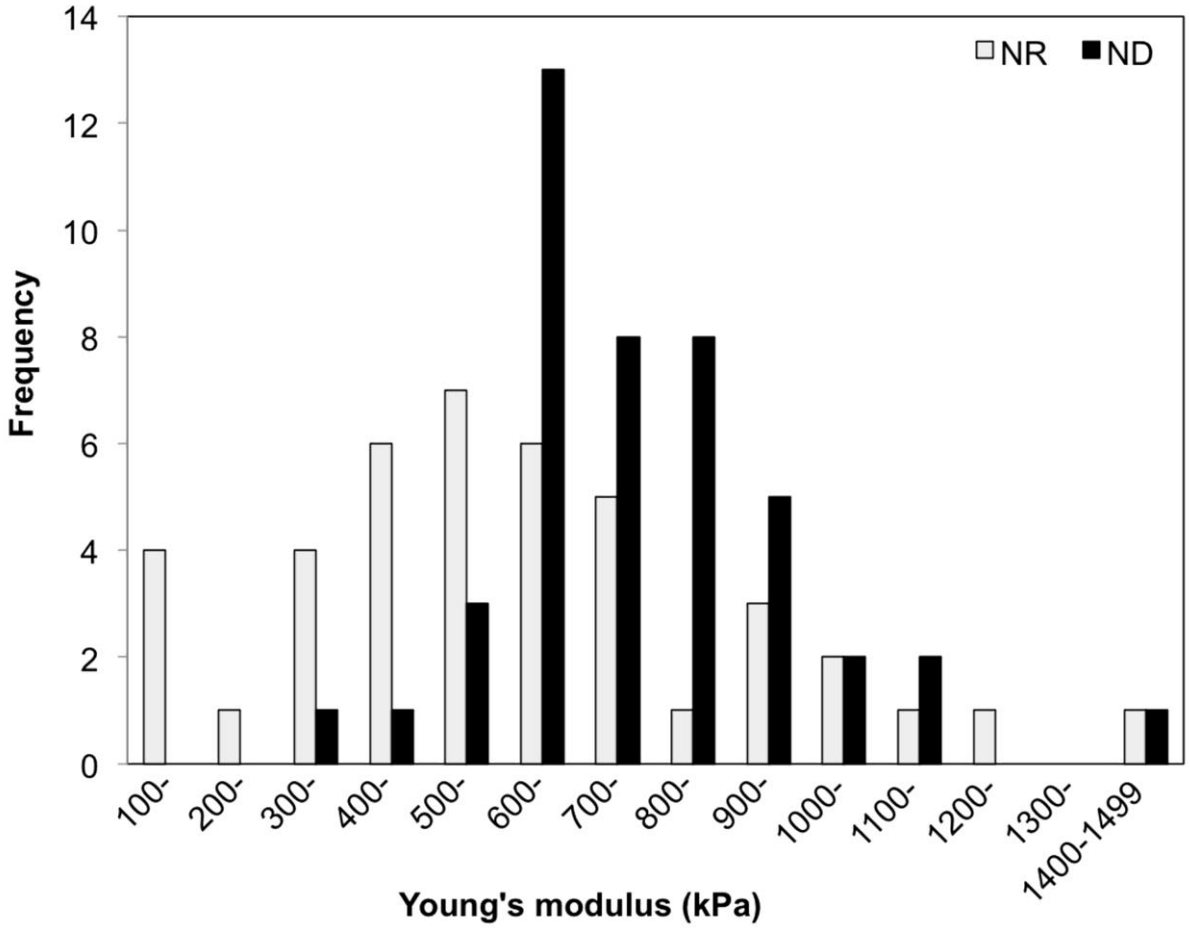
NR
ND
Frequency
Young's modulus (kPa)
100-
200-
300-
400-
500-
600-
700-
800-
900-
1000-
1100-
1200-
1300-
1400-1499

558

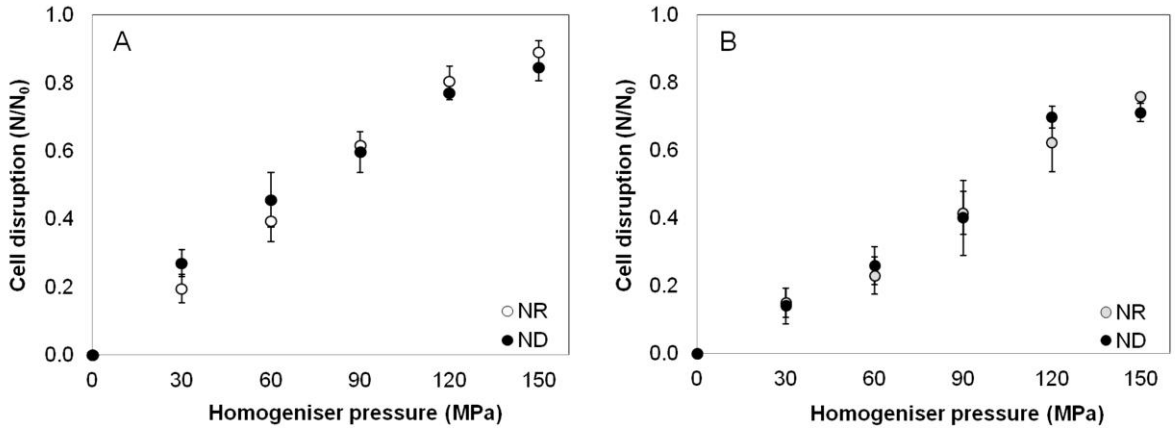

559

560 Table Mean cell wall thickness and cell size of *Nannochloropsis* sp., *Chlorella* sp. and
561 *Chlorococcum* sp. grown in N-replete (NR) and N-deplete (ND) conditions. Cell wall of individual
562 cells was measured in 3-5 separate places and a total of 20-35 cells per species were measured. Mean
563 values are within the given standard deviation with >99% confidence level with *p*-values for all
564 parameters calculated to be <0.0001.

Microalgae	Growth condition	Mean cell wall thickness, CW (nm)	Mean cell size, CS (μm)	CW/CS ($\times 10^{-3}$)
Nannochloropsis sp.	NR	12 ± 2	2.0 ± 0.1	5.7
	ND	15 ± 2	2.5 ± 0.2	6.0
Chlorella sp.	NR	52 ± 19	2.4 ± 0.1	22.0
	ND	88 ± 17	2.9 ± 0.2	30.6
Chlorococcum sp.	NR	387 ± 90	9.4 ± 1.1	41.2
	ND	503 ± 67	12.9 ± 2.1	39.2

565

566

567